

Aberrant expression of two miRNAs promotes proliferation, hepatitis B virus amplification, migration and invasion of hepatocellular carcinoma cells: evidence from bioinformatic analysis and experimental validation

Yanming Liu^{1,2}, Yue Cao³, Wencan Cai², Liangyin Wu², Pingsen Zhao² and Xin-guang Liu¹

¹ Guangdong Provincial Key Laboratory of Medical Molecular Diagnostics, Institute of Aging Research, Guangdong Medical University, Dongguan, Guangdong, China

² Department of Clinical Laboratory, YueBei People's Hospital, Shaoguan, Guangdong, China

³ Department of Medical Technology, Medical College of Shaoguan University, Shaoguan, Guangdong, China

ABSTRACT

Background: As key negative regulators of gene expression, microRNAs (miRNAs) play an important role in the onset and progression of hepatocellular carcinoma (HCC). This study aimed to identify the miRNAs involved in HCC carcinogenesis and their regulated genes.

Methods: The Gene Expression Omnibus (GEO) dataset ([GSE108724](#)) was chosen and explored to identify differentially expressed miRNAs using GEO2R. For the prediction of potential miRNA target genes, the miRTarBase was explored. Enrichment analysis of Gene Ontology (GO) and the Kyoto Encyclopedia of Genes and Genomes (KEGG) was performed by the DAVID online tool. The hub genes were screened out using the CytoHubba plug-in ranked by degrees. The networks between miRNAs and hub genes were constructed by Cytoscape software. MiRNA mimics and negative control were transfected into HCC cell lines and their effects on proliferation, hepatitis B virus DNA (HBV-DNA) replication, *TP53* expression, migration, and invasion were investigated. The following methods were employed: MTT assay, quantitative PCR (qPCR) assay, western blotting, wound healing assay, and transwell assay.

Results: A total of 50 differentially expressed miRNAs were identified, including 20 upregulated and 30 downregulated miRNAs, in HCC tumor tissues compared to matched adjacent tumor-free tissues. The top three upregulated (miR-221-3p, miR-222-3p, and miR-18-5p) and downregulated (miR-375, miR-214-3p and miR-378d) miRNAs, ranked by $|\log_2 \text{fold change} (\log_2 \text{FC})|$, were chosen and their potential target genes were predicted. Two gene sets, targeted by the upregulated and the downregulated miRNAs, were identified respectively. GO and KEGG pathway analysis showed that the predicted target genes of upregulated and downregulated miRNAs were mainly enriched in the cell cycle and cancer-related pathways. The top ten hub nodes of gene sets ranked by degrees were identified as hub genes. Analysis of

Submitted 13 December 2019

Accepted 9 April 2020

Published 29 April 2020

Corresponding author

Xin-guang Liu, xgliu@gdmu.edu.cn

Academic editor

Vladimir Uversky

Additional Information and
Declarations can be found on
page 16

DOI [10.7717/peerj.9100](https://doi.org/10.7717/peerj.9100)

© Copyright
2020 Liu et al.

Distributed under
Creative Commons CC-BY 4.0

OPEN ACCESS

miRNA-hub gene network showed that miR-221-3p and miR-375 modulated most of the hub genes, especially involving regulation of TP53. The q-PCR results showed that miR-221-3p and miR-375 were markedly upregulated and downregulated, respectively, in HCC cells and HCC clinical tissue samples compared to non-tumoral tissues. Furthermore, miR-221-3p overexpression significantly enhanced proliferation, HBV-DNA replication, as well as the migration and invasion of HCC cells, whereas miR-375 overexpression resulted in opposite effects. Western blotting analysis showed that the overexpression of miR-221-3p and miR-375 reduced and increased TP53 expression, respectively.

Conclusion: The present study revealed that miR-221-3p and miR-375 may exert vital effects on cell proliferation, HBV-DNA replication, cell migration, and invasion through the regulation of TP53 expression in HCC.

Subjects Bioinformatics, Gastroenterology and Hepatology, Oncology

Keywords microRNA, Hepatocellular carcinoma, Bioinformatic analysis, Invasion, HBV amplification, Proliferation

INTRODUCTION

With the second-highest morbidity, third-highest mortality rate, and fifth-highest global incidence in China, hepatocellular carcinoma (HCC) is one of the most lethal malignant tumors, and new cases are increasing worldwide each year ([Yanming et al., 2019](#)).

The risk factors for HCC are mainly represented by chronic hepatitis B virus (HBV) or hepatitis C virus (HCV) infection, cirrhosis, and alcoholic liver disease ([Xie et al., 2019](#); [Zhang et al., 2019](#)). Alpha-fetoprotein (AFP), the most important tumor marker for HCC diagnosis, has been used for decades but results in a clinically unsatisfactory sensitivity of 40–65% and a specificity of 76–96% ([Yanming et al., 2019](#)). Therefore, the identification of novel biomarkers of HBV replication and HCC proliferation, migration, and invasion is urgent and crucial for developing effective diagnostic, therapeutic, and prognostic follow-up strategies. MicroRNAs (miRNAs) are endogenous 21–25 nt RNAs that induce mRNA degradation or inhibition of translation by binding to the 3'-untranslated region of target messenger RNAs (mRNAs). It has been demonstrated that the abnormal expression of specific miRNAs promotes the proliferation, invasion, and metastasis of tumor cells ([Wang et al., 2018](#)). Therefore, thorough investigation of miRNAs that are functionally related to HBV-infection, as well as to the proliferation, migration, and invasion of HCC cells is of paramount importance.

High-throughput microarray technology has been extensively applied for decades owing to its high sensitivity and processivity. Bioinformatic analysis is widely used to identify differentially expressed miRNAs (DE-miRNAs) and functional pathways involved in carcinogenesis and HCC progression. The combination of these two approaches may help understand the pathogenesis of tumors and improve early diagnosis, treatment, and prognosis of HCC patients ([Mantione et al., 2014](#)).

In the present study, the [GSE108724](#) dataset, comprising seven pairs of HCC and matched adjacent tumor-free tissues, was applied to the screening of 50 differentially

expressed miRNAs (DE-miRNAs), including 20 upregulated and 30 downregulated miRNAs related to HCC pathogenesis. The top three upregulated and downregulated miRNAs, ranked by $|\log_2 \text{fold change} (\log_2 \text{FC})|$, were selected to predict potential target genes, respectively. Enriched Gene Ontology (GO) terms and Kyoto Encyclopedia of Genes and Genomes (KEGG) pathways of each gene set were identified using the DAVID online tool. Protein-protein interaction (PPI) networks were constructed to identify the top ten hub nodes of each gene set, ranked by degrees as hub genes, using the CytoHubba plug-in. Then, the networks established by the top three upregulated and downregulated miRNAs with their 10 target hub genes were constructed. MiR-221-3p and miR-375 exhibited the most regulatory relationships with their hub genes, with special regard to *TP53* regulation. Subsequently, in vitro validation experiments were performed. As the novelty and innovation of this present research, bioinformatics and experimental validation were combined to explore the effects of miR-211-3p and miR-375 on HBV DNA amplification, *TP53* expression, as well as on the proliferation, migration, and invasion of HCC cell lines.

MATERIALS AND METHODS

Microarray data

To explore the role of specific miRNAs in HCC pathogenesis, the [GSE108724](#) dataset ([Zhu et al., 2019](#)) was selected and downloaded from GEO (<https://www.ncbi.nlm.nih.gov/geo/>). This dataset, based on the [GPL20712](#) platform (Agilent-070156 Human miRNA), contained miRNA expression profiles of 7 pairs of HCC and matched adjacent tumor-free tissues.

DE-miRNA identification and target gene prediction

The DE-miRNAs between HCC and matched adjacent tumor-free tissues were screened using GEO2R (<http://www.ncbi.nlm.nih.gov/geo/geo2r>) according to the cut-off criterion that $P\text{-value} < 0.05$ and $|\log_2 \text{fold change} (\log_2 \text{FC})| > 2$, an online interactive web tool with built-in GEOquery and limma R packages that allows to compare two or more datasets across experimental conditions. The GEOquery R package parses GEO data into R data structures that can be used by other R packages ([Davis & Meltzer, 2007](#)). The Limma R package is used to homogenize microarray data and to reduce the occurrence of false positives by applying multiple-testing corrections on P -values ([Ritchie et al., 2015](#)). The miRTarBase online dataset (<http://mirtarbase.mbc.nctu.edu.tw/php/index.php>) (version 7.0), containing extensive information on experimentally validated miRNA-target interactions, was utilized for predicting potential miRNA target genes ([Chou et al., 2018](#)). Only the top three upregulated and downregulated miRNAs, ranked by $|\log_2 \text{FC}|$, were enrolled for target gene prediction analysis and formed two new gene sets of upregulated and downregulated miRNAs, on which GO, KEGG, and hub gene identification analyses were further performed.

GO, KEGG, hub gene identification and miRNA-hub gene network construction

The Database for Annotation, Visualization and Integrated Discovery (DAVID; <https://david.ncifcrf.gov>) (version 6.8) ([Da Huang, Sherman & Lempicki, 2009a, 2009b](#)),

providing a comprehensive set of functional annotation information including large lists of genes, allowing for the retrieval of biological information, was applied to perform functional annotation and pathway enrichment analysis for the two gene sets, including GO (Edgar, Domrachev & Lash, 2002) and KEGG (Kanehisa et al., 2017) pathway analysis. Search Tool for the Retrieval of Interacting Genes (STRING) (<https://string-db.org/>) is the most popular database of known and predicted protein–protein interactions (PPI). The PPI networks of the two gene sets were constructed using STRING (version 11.0), and interactions with a combined score >0.4 were considered statistically significant (Szklarczyk et al., 2019). The top ten hub genes of the two gene sets ranked by degrees were selected by using the CytoHubba plug-in (<http://apps.cytoscape.org/apps/cytohubba>) (version 0.1) (Chin et al., 2014). The Cytoscape software (<https://cytoscape.org>) (version 3.7.2) was used to construct the networks between three miRNAs and their respective top ten hub target genes (Shannon et al., 2003). *P*-value < 0.05 was considered as statistically significant.

Analysis of gene and miRNA expression, survival, and co-expression of miRNAs-hub genes

The Cancer Genome Atlas (TCGA) analysis tool of the UALCAN database (<http://ualcan.path.uab.edu/>), an interactive web resource for the analysis of cancer omics data, was utilized to explore differences in the expression of hub genes between normal and tumor tissue in patients with liver hepatocellular carcinoma (LIHC) (Chandrashekar et al., 2017). The OncomiR database (<http://www.oncomir.org/>), an online resource for the evaluation of cancer-related miRNA dysregulation, was applied for performing Kaplan–Meier survival analysis based on the expression level of miR-221-3p and miR-375, with 50% as percentile cutoff value in HCC (Wong et al., 2018). The Pan-Cancer analysis tool of starBase (version 3.0) (<http://starbase.sysu.edu.cn/panMirCoExp.php>), identifying more than 2.5 million miRNA–mRNA interactions from multi-dimensional sequencing data, was used for miRNA–target gene co-expression analysis (Li et al., 2014). *P*-value of < 0.05 was considered as statistically significant.

HCC cell lines, clinical samples, and cell transfection

Immortalized normal human liver HL7702 cells and the HCC cell lines HepG2, HepG2.2.15, and MHCC-LM3 were purchased from Cellcook Co., Ltd. (Guangzhou, China). All cells were cultured in Dulbecco’s modified Eagle’s medium/High Glucose (DMEM: 8885329; Gibco, Shanghai, China) with 10% fetal bovine serum (FBS: 11011-8611; Tianhang, Hangzhou, China) and maintained under a humidified atmosphere of 5% CO₂ at 37 °C. With the written informed consent from participants and the approval obtained from the institutional ethics review board of YueBei people’s Hospital (approval number: SUMC-IRB-2017), HCC tumor tissues and matched adjacent tumor-free tissues were obtained from YueBei People’s Hospital. According to the manufacturer’s instructions, the riboFECT CP Transfection Kit (C10511-05; RiboBio, Guangzhou, China) was used to transfect miRNA mimics and negative control (RiboBio, Guangzhou, China) into HCC cell lines.

RNA isolation and quantitative reverse transcription PCR

Total RNA from different cell lines and human tissues was extracted using the RNA Extraction Kit (R1405; GBCBIO, Guangzhou, China). The extracted RNA was stored at -80°C after measuring the concentration and quality. Stem-loop reverse transcriptase (RT) primers for two miRNAs were designed and purchased from TSINGKE Biological Technology Co., Ltd., Beijing, China. Q-PCR was performed three times using SYBR Premix Ex Taq (Q111-02; Vazyme, Nanjing, China) and normalized with U6 small nuclear RNA as internal reference. The $2^{-\Delta\Delta\text{CT}}$ method was applied to determine the relative expression level of miRNAs. The sequences of qRT-PCR primers are shown in [Table S1](#).

MTT cell proliferation assay

HepG2 cells (2×10^3 cells/well) were plated in 96-well plates. After transfection (final transfection concentration of miRNA mimics and negative control: 50 nM) and growth to 95% confluence, HepG2 cells were harvested. Cell proliferation was analyzed in triplicate by using the MTT assay kit (G7420-2; GBCBIO, Guangzhou, China) according to the manufacturer's instruction.

HBV-DNA qPCR detection

HepG2.2.15 cells (1×10^5 cells/well) were seeded in 6-well plates. After transfection, the HBV-DNA quantitative kit (2019005; DAAN Gene, Guangzhou, China), including the reagents for DNA extraction, PCR amplification, calibration, and quality control, was used for measuring the level of HBV-DNA in one mL of cell culture supernatant, as per manufacturer's instructions.

Western blot

Western blot was performed as previously described with minor modifications ([Marangos, 2016](#)). HepG2 cells (1×10^5 cells/well) were seeded in 6-well plates. After transfection and growth to 95% confluence, the cells were harvested. The following primary antibodies were used: anti-p53 (ab131442; Abcam, Cambridge, UK, 1:100) and anti-GAPDH (EPR16891; Abcam, Cambridge, UK, 1:100). The horseradish peroxidase-labeled secondary antibody ab205718, Abcam, Cambridge, UK was used (1:500). A DAB Horseradish Peroxidase Color Development Kit (G3433; GBCBIO, Guangzhou, China) was employed to visualize p53 and GAPDH. The colored bands on the PVDF membrane were photographed with an OLYMPUS microscope (Tokyo, Japan) and permanently stored.

Wound healing assays

HepG2 cells (1×10^5 cells/well) were seeded in 12-well plates. After transfection and growth to 95% confluence, a sterilized pipette tip was used to scratch a wound. The wounded areas were photographed with a microscope, immediately and after 24 h (magnification: 100 \times).

Transwell assay

The cell invasion assay was performed using 24-well transwell chambers (3422; Corning Inc., New York, USA). The transwell chamber (upper compartment) was separated from the 24-well plate (lower compartment) by polycarbonate membrane with a pore size of 8 μm . The upper surface of the polycarbonate membrane was coated with Matrigel (354230; BD Bioscience, San Jose, CA, USA, 1:8 dilution). After transfection, 200 μL of serum-free medium containing 1×10^5 HepG2 cells were added to the upper compartment. Next, 600 μL of medium containing 20% FBS were added to the lower compartment. Then, after a 24-h incubation at 37 °C and removal of the cells on the upper surface of the membrane in the upper compartment using a cotton bud, the membranes were fixed (95% methanol) for 30 min, stained (0.1% crystal violet) for 20 min at room temperature, and three visual fields were photographed (magnification: 200 \times) under a microscope (OLYMPUS, Tokyo, Japan). The experiments were independently repeated in triplicate.

Statistical analysis

The results were expressed as mean \pm SD. The raw data obtained with the HBV-DNA assay were subjected to base 10 logarithmic conversion before statistical analysis. One-way ANOVA analysis was used to compare the miRNA expression between four cell lines. The two-independent *t*-test was used to compare miRNAs expression between para-tumor and tumor tissues. Unless otherwise noted, statistical diagrams were drawn using GraphPad Prism (version 8.0.1; GraphPad Software, San Diego, CA, USA). For all analyses, $P < 0.05$ was regarded as statistically significant.

RESULTS

Identification of DE-miRNAs and of their potential target genes in HCC

The GEO2R online tool was applied to screen 50 DE-miRNAs between 7 HCC tissues and their matched adjacent tumor-free tissues in the [GSE108724](#) dataset (P -value < 0.05 and $|\log_2\text{FC}| > 2$). Twenty upregulated and thirty downregulated DE-miRNAs are shown in the volcano plot ([Fig. 1](#)). [Tables 1](#) and [2](#) show the top ten upregulated and downregulated DE-miRNAs, respectively, ranked by $|\log_2\text{FC}|$. A total of 741 potential target genes were predicted for the top three upregulated miRNAs (miR-221-3p, and miR-222-3p, and miR-18b-5p), while 696 genes were identified as candidate targets of the top three downregulated miRNAs (miR-375, miR-214-3p, and miR-378d) by using the miRTarBase online tool.

Functional enrichment analysis of target genes

To comprehensively investigate the biological functions of target genes, GO and KEGG pathway enrichment analyses were carried out using the DAVID online tool. GO analysis can be divided into three functional groups: biological process group (BP), molecular function group (MF), and cellular component group (CC). GO analysis of the 741 potential target genes of the three upregulated miRNAs revealed that changes in BP were mainly enriched in negative regulation of transcription from RNA polymerase II

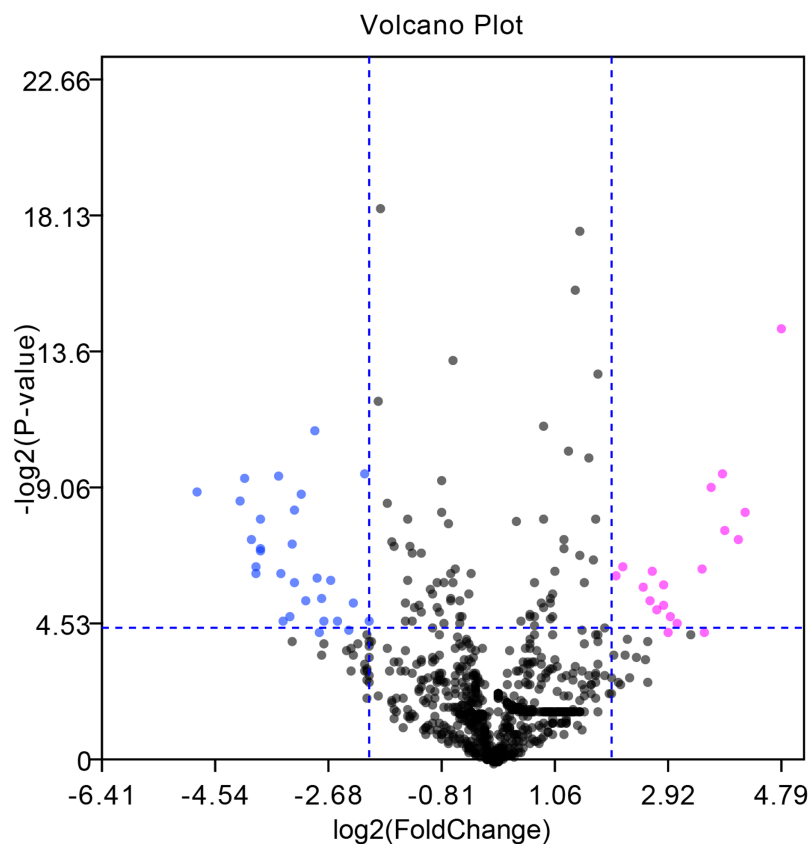


Figure 1 Volcano plot of DE-miRNAs between seven pairs of HCC and matched adjacent tumor-free tissues in the GSE108724 dataset. Red and green dots represent upregulated and downregulated miRNAs, respectively, based on P -value < 0.05 and $|\log_2FC| > 2$; black dots represent miRNAs with no significant expression differences. [Full-size](#) DOI: 10.7717/peerj.9100/fig-1

Table 1 The top ten upregulated miRNAs between HCC and matched adjacent tumor-free tissues ranked by $|\log_2FC|$.

ID	\log_2FC	P -value	t	B
hsa-miR-221-3p	3.75	1.27E-03	4.10	-0.73
hsa-miR-222-3p	3.57	1.70E-03	3.95	-0.99
hsa-miR-18b-5p	3.41	1.12E-02	2.96	-2.70
hsa-miR-500a-3p	2.80	2.57E-02	2.52	-3.44
hsa-miR-196b-5p	2.80	1.62E-02	2.77	-3.03
hsa-miR-7-5p	2.60	1.21E-02	2.92	-2.77
hsa-miR-6516-3p	2.55	2.39E-02	2.56	-3.38
hsa-miR-34a-3p	2.46	1.72E-02	2.73	-3.09
hsa-miR-362-3p	2.13	1.08E-02	2.97	-2.67
hsa-miR-339-3p	2.02	1.35E-02	2.86	-2.87

Table 2 The top ten downregulated miRNAs between HCC and matched adjacent tumor-free tissues ranked by $|\log_2FC|$.

ID	Log ₂ FC	P value	t	B
hsa-miR-375	-6.41	1.51E-07	-10.22	6.72
hsa-miR-214-3p	-4.90	1.94E-03	-3.88	-1.11
hsa-miR-378d	-4.20	2.38E-03	-3.77	-1.30
hsa-miR-486-5p	-4.13	1.37E-03	-4.06	-0.80
hsa-miR-199a-5p	-3.86	3.51E-03	-3.56	-1.65
hsa-miR-8089	-3.54	1.34E-03	-4.08	-0.77
hsa-miR-338-3p	-3.28	2.91E-03	-3.66	-1.48
hsa-miR-7845-5p	-3.20	1.98E-03	-3.87	-1.13
hsa-miR-199a-3p	-2.95	4.74E-04	-4.64	0.16
hsa-miR-10a-5p	-2.13	1.23E-03	-4.12	-0.70

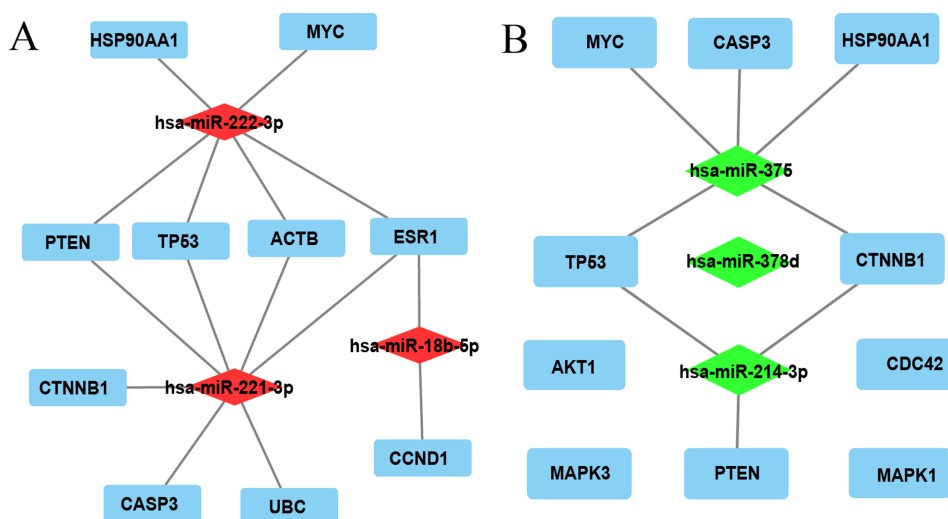
promoter, positive regulation of transcription, and cell-cell adhesion (Fig. S1A); changes in MF were mainly enriched in poly(A) RNA binding, protein binding, and cadherin binding involved in cell-cell adhesion (Fig. S1C); changes in CC were mainly enriched in nucleoplasm, nucleus, and cytosol (Fig. S1E). GO analysis of the 696 target genes of the three downregulated miRNAs revealed that changes in BP were mainly involved positive regulation of neuron apoptotic process, organ morphogenesis, and blood vessel remodeling (Fig. S1B); changes in MF were mainly involved GDP binding, transcription coactivator activity, and mRNA binding (Fig. S1D); changes in CC were mainly involved nucleus, extracellular exosome, and nucleoplasm (Fig. S1F). KEGG pathway analysis showed that the 741 candidate target genes of the three upregulated miRNAs were mainly enriched in cell cycle, cancer-related pathways, and FoxO signaling pathway (Fig. S1G); the 696 target genes of the three downregulated miRNAs were mainly involved cancer-related pathways, breast cancer, hepatitis B, and MAPK signaling pathway (Fig. S1H).

Hub gene identification, miRNA-hub gene network construction, and targeted gene expression analysis in HCC tissues

The top 10 nodes ranked by degrees of the CytoHubba plug-in of Cytoscape software were recognized as hub genes. Six (*TP53*, *MYC*, *HSP90AA1*, *PTEN*, *CASP3*, *CTNNB1*) of ten hub genes were in common between upregulated and downregulated DE-miRNAs, albeit they exhibited different scores (Table 3). *TP53*, exhibiting the highest score among upregulated and downregulated DE-miRNAs, could play a vital role in HCC carcinogenesis or progression. The analysis of the miRNA-Hub gene network revealed that miR-221-3p potentially modulated seven (*PTEN*, *TP53*, *ACTB*, *ESR1*, *CTNNB1*, *CASP3*, and *UBC*) of ten hub genes. Moreover, miR-222-3p and miR-18b-5p regulated six and two hub genes, respectively (Fig. 2A). Interestingly, miR-375 potentially modulated five (*HSP90AA1*, *CASP3*, *MYC*, *TP53*, and *CTNNB1*) of 10 hub genes. MiR-214-3p and miR-378d could regulate three and zero hub genes, respectively (Fig. 2B).

Table 3 The top ten hub genes of target gene sets predicted by three upregulated and downregulated miRNAs ranked by degrees.

Upregulated DE-miRNAs			Downregulated DE-miRNAs		
Rank	Name	Score	Rank	Name	Score
1	<i>TP53</i>	172	1	<i>TP53</i>	151
2	<i>MYC</i>	128	2	<i>AKT1</i>	141
3	<i>HSP90AA1</i>	108	3	<i>MYC</i>	107
3	<i>UBC</i>	105	4	<i>PTEN</i>	90
5	<i>PTEN</i>	104	5	<i>MAPK3</i>	87
6	<i>CCND1</i>	91	6	<i>HSP90AA1</i>	84
7	<i>CASP3</i>	82	7	<i>CTNNB1</i>	83
8	<i>CTNNB1</i>	82	8	<i>CDC42</i>	82
9	<i>ESR1</i>	81	9	<i>MAPK1</i>	77
10	<i>ACTB</i>	79	10	<i>CASP3</i>	76

**Figure 2** The miRNA-hub gene network was constructed using Cytoscape software. (A) Network of three upregulated miRNAs and their predicted hub genes. (B) Network of three downregulated miRNAs and their predicted hub genes. Red diamonds represent upregulated miRNAs, green diamonds represent downregulated miRNAs, cyan rectangles represent hub genes, lines represent the interaction between miRNAs and hub genes, and free diamonds and rectangle represent the absence of interaction between miRNAs and hub genes. [Full-size !\[\]\(c1a2abfc6348d89531e4a1cc1534ae43_img.jpg\) DOI: 10.7717/peerj.9100/fig-2](https://doi.org/10.7717/peerj.9100/fig-2)

Eleven significantly upregulated hub genes (*UBC*, *ACTB*, *TP53*, *HSP90AA1*, *PTEN*, *CASP3*, *CTNNB1*, *AKT1*, *MAPK3*, *CDC42*, and *MAPK1*) (Figs. 3A, 3D, 3E, 3I–3P) and two significantly downregulated hub genes (*ESR1* and *MYC*) (Figs. 3C and 3H) were compared in HCC tissues and normal liver tissues using the TCGA analysis tool of the UALCAN database. The results of TCGA analysis showed that the expression level of *TP53* was positively related to HCC tumor stage and metastasis (Figs. 3F and 3G). *TP53*, one of the hub genes in common between the two sets of DE-miRNAs, exhibiting the highest score,

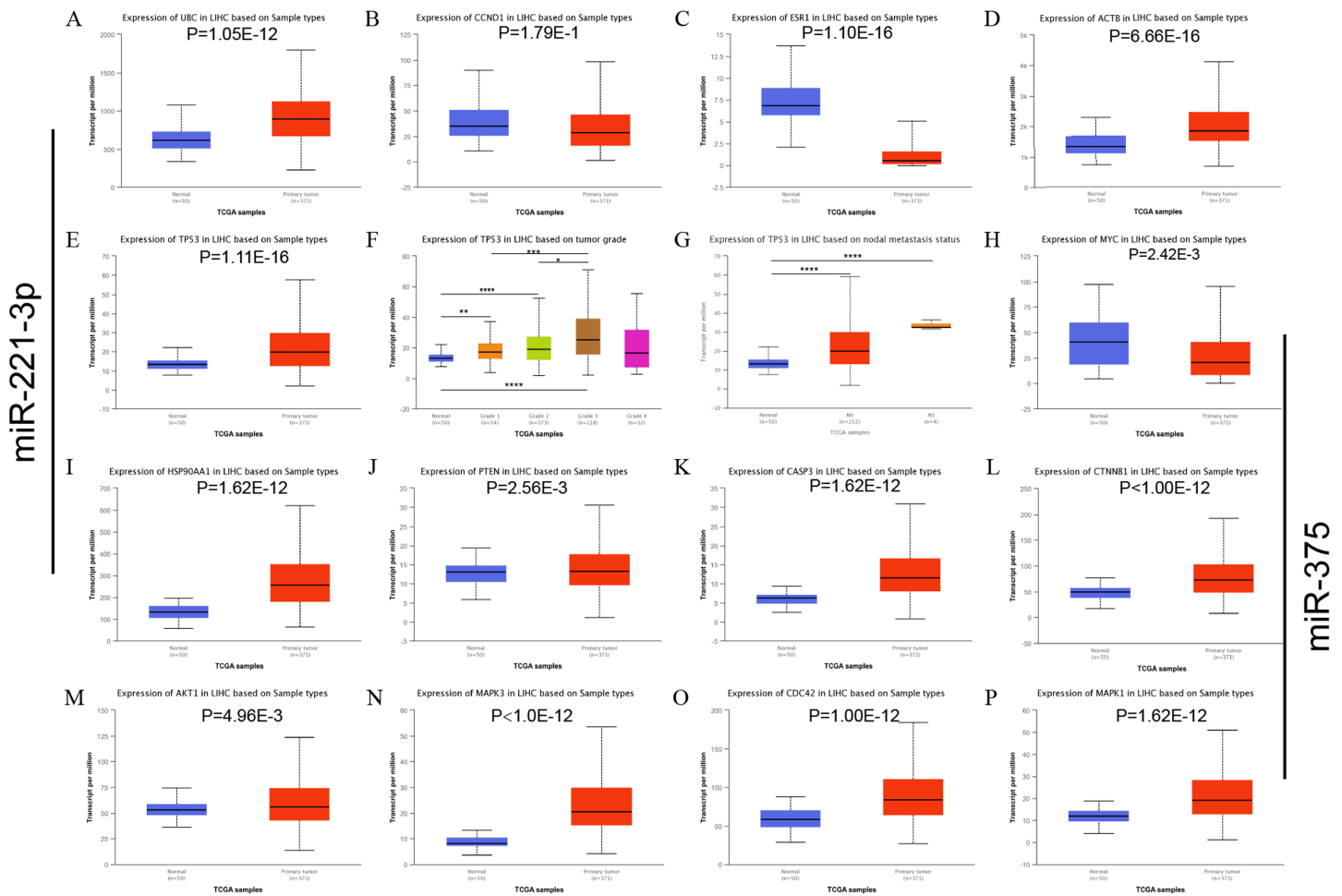


Figure 3 mRNA expression of the predicted hub genes of miR-221-3p and miR-375 from the UALCAN LHC database. The hub genes were potential predictive targets of miR-221-3p (A–L) and miR-375 (E–P). (A) UBC expression based on sample type. (B) CCND1 expression based on sample type. (C) ESR1 expression based on sample types. (D) ACTB expression based on sample types. (E) TP53 expression based on sample types. (F) TP53 expression based on tumor grade. (G) TP53 expression based on nodal metastasis status. (H) MYC expression based on sample type. (I) HSP90AA1 expression based on sample type. (J) PTEN expression based on sample type. (K) CASP3 expression based on sample type. (L) CTNNB1 expression based on sample type. (M) AKT1 expression based on sample type. (N) MAPK3 expression based on sample type. (O) CDC42 expression based on sample type. (P) MAPK1 expression based on sample type. * $P < 0.05$; ** $P < 0.01$; *** $P < 0.001$; **** $P < 0.0001$.

Full-size [DOI: 10.7717/peerj.9100/fig-3](https://doi.org/10.7717/peerj.9100/fig-3)

maybe the most potentially hub gene of miR-221-3p and miR-375. Based on the above findings, we speculated that miR-221-3p and miR-375 might play critical roles in HCC by regulating *TP53* expression.

The expression level of miR-221-3p and miR-375 in HCC cells and clinical samples

Three HCC cell lines (HepG2, HepG2.2.15, and HCC-LM3) and a normal liver cell line (HL7702) were employed to evaluate the expression level of miR-221-3p and miR-375. qRT-PCR revealed that the two miRNAs were significantly upregulated and downregulated in all three HCC cell lines, respectively, compared to HL7702 cells (Figs. 4A and 4D). Notably, the expression levels of miR-221-3p and miR-375 were the

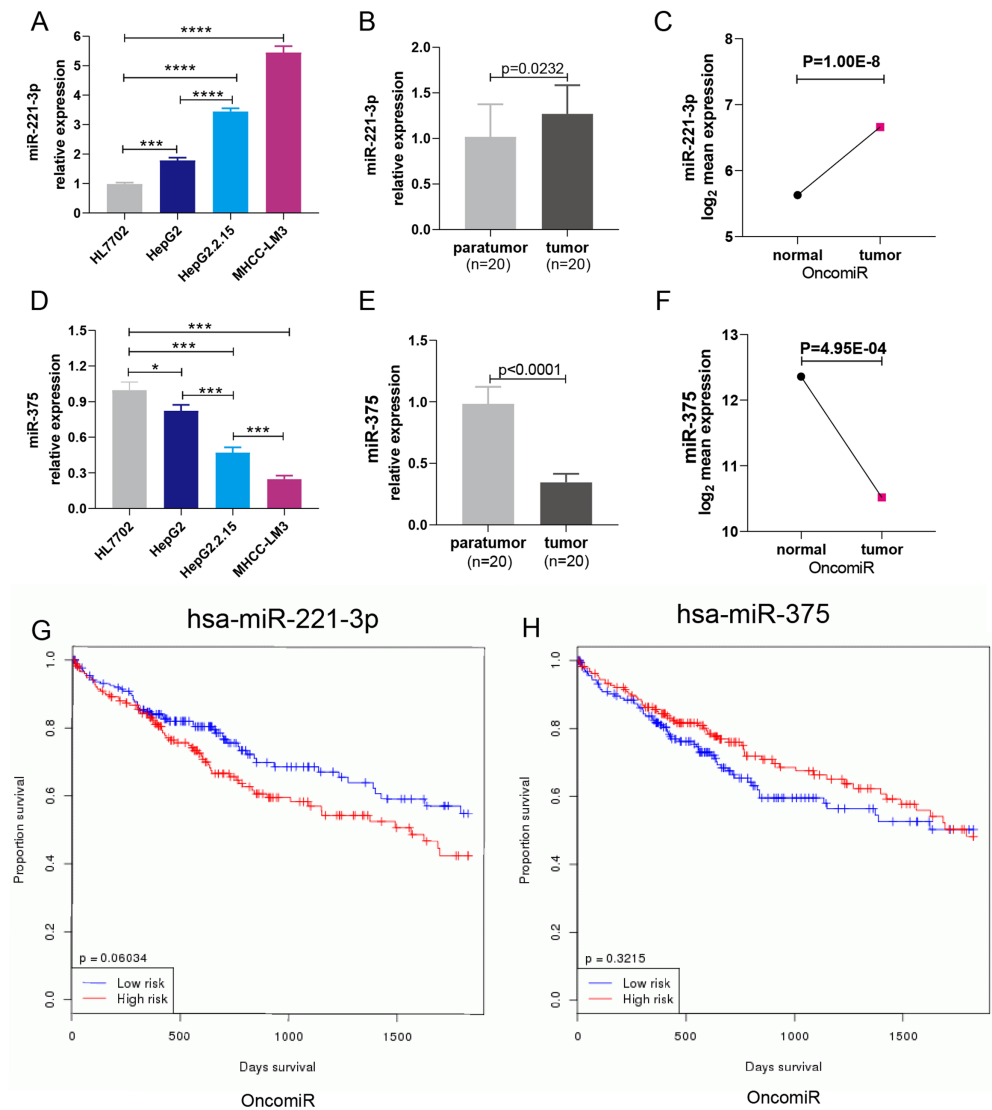


Figure 4 The expression and prognostic roles of miR-221-3p and miR-375 in HCC. The expression level of miR-221-3p (A) and miR-375 (D) in three HCC cell lines (HepG2, HepG2.2.15, MHCC-LM3) and one normal liver cell line (HL7702) detected by qRT-PCR. MiR-221-3p and miR-375 were significantly upregulated and downregulated in all three HCC cell lines, respectively, compared to HL7702 cells. The expression level of miR-221-3p (B) and miR-375 (E) in 20 clinical HCC samples vs matched para-tumor tissues detected by qRT-PCR. MiR-221-3p and miR-375 were, respectively, upregulated and downregulated in 20 HCC tissue samples compared to their para-tumor tissues. The mean expression level of miR-221-3p (C) and miR-375 (F) in multiple clinical HCC samples vs normal tissues, as assessed by OncomiR online analysis. The mean expression level of miR-221-3p and miR-375 in multiple clinical HCC samples was much higher and lower, respectively, than that of normal tissues. Kaplan-Meier survival curve of miR-221-3p (G) and miR-375 (H) based on percentile cutoff value 50% in HCC, as determined by OncomiR online analysis. high miR-221-3p expression and low miR-375 expression tended to be correlated with poor overall survival. However, this association was not statistically significant ($P = 0.06034$ for miR-221-3p and $P = 0.3215$ for miR-375). The cohort labeled as high-risk (red line) represents levels of miRNA expression above the average level; the cohort labeled as low-risk (blue line) represents miRNA expression levels below the average level. One-way ANOVA analysis was used to compare the miRNA expression between four cell lines. The two-independent t -test was used to compare miRNAs expression between para-tumor and tumor tissues. * $P < 0.05$; *** $P < 0.001$; **** $P < 0.0001$.

Full-size DOI: 10.7717/peerj.9100/fig-4

highest and lowest in HCC-LM3 compared to the other two HCC cell lines, respectively. Due to the high invasion capacity of HCC-LM3 cells (Zha *et al.*, 2018), this suggested that miR-221-3p and miR-375 could be critical regulators of HCC cell invasion. HepG2.2.15 is an HCC cell line that carries and secretes HBV particles. Notably, in these cells, miR-221-3p expression was much higher, and that of miR-375 much lower, compared to HepG2 cells. These findings were consistent with an important role of miR-221-3p and miR-375 in the tumorigenesis of HBV-related HCC. Subsequently, qRT-PCR analysis of HCC tissue samples demonstrated that miR-221-3p and miR-375 were, respectively, upregulated and downregulated in 20 HCC tissue samples compared to their para-tumor tissues (Figs. 4B and 4E). Next, the OncomiR online database was employed to further evaluate the expression level and the prognostic value of miR-221-3p and miR-375 in HCC patients. The mean expression level of miR-221-3p was much higher, and that of miR-375 much lower, in HCC tissues compared to normal liver tissues (Figs. 4C and 4F). Interestingly, high miR-221-3p expression and low miR-375 expression tended to be correlated with poor overall survival. However, this association was not statistically significant ($P = 0.06034$ for miR-221-3p and $P = 0.3215$ for miR-375) (Figs. 4G and 4H). In conclusion, although further experimental validation is needed, miR-221-3p and miR-375 are potential prognostic biomarkers, with special regard to HBV amplification and HCC invasion.

The effects of miR-221-3p and miR-375 overexpression on proliferation, HBV-DNA replication, migration, and invasion of HCC cells

HepG2 cells were transfected with 50 nM or 100 nM miRNA mimics. qRT-PCR analysis showed that miRNA expression increased with the concentration of transfected miRNA mimics (Fig. 5A). After experimental verification, 50 nM was selected as the most suitable concentration of the two miRNAs for subsequent transfections. First, we performed an MTT assay to explore the impact of miR-221-3p and miR-375 on HCC cell proliferation. The results showed that miR-221-3p and miR-375 overexpression significantly enhanced and decreased, respectively, HepG2 cell proliferation when compared to HepG2 cells transfected with the negative control (Fig. 5B). In addition, we performed an HBV-DNA qPCR assay to determine the effect of miR-221-3p and miR-375 overexpression on the replication of HBV-DNA. The qPCR results showed that the upregulation of miR-221-3p and miR-375 increased and decreased, respectively, the level of HBV-DNA in HepG2.2.15 cells (Fig. 5C). Moreover, western blot analysis indicated that miR-221-3p and miR-375 overexpression weakened and enhanced, respectively, the expression of *TP53* (Fig. 5D). The co-expression experiments showed that the level of *TP53* expression was strongly correlated with those of the two miRNAs in HCC patients (miR-221-3p: $r = 0.313$, P -value: $7.16E-10$; miR-375: $r = 0.036$, P -value: $4.59E-1$) (Figs. 5E and 5F). Moreover, we performed a wound healing assay to evaluate the role of miR-221-3p and miR-375 in HCC cell migration. HepG2 cell migration was positively correlated with miR-221-3p overexpression and negatively correlated with miR-375 overexpression (Figs. 6A and 6B). Finally, the effects of the two miRNAs on HCC cell

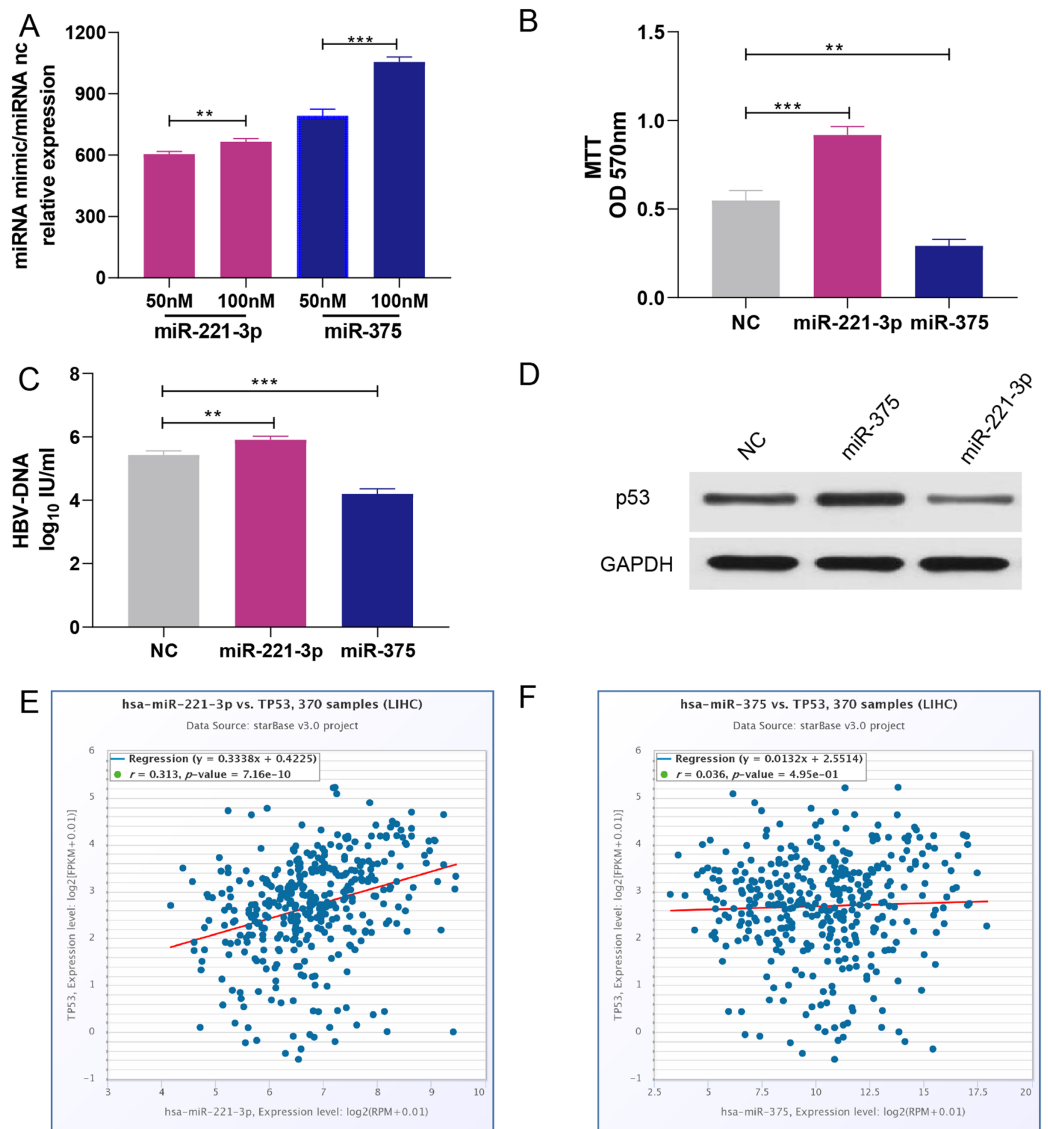


Figure 5 Overexpression of miR-221-3p and miR-375 affect cell proliferation, HBV-DNA replication, and TP53 expression in HCC cell lines. (A) The relative expression level of miR-221-3p/NC and miR-375/NC after transfection with NC, miR-221-3p mimics, and miR-375 mimics (at the final concentrations of 50 nM or 100 nM) in HepG2 cells. The miRNA mimics (miR-221-3p and miR-375) significantly increased the expression of the corresponding miRNAs at both concentrations. (B) The overexpression of miR-221-3p and miR-375 in HepG2 cells enhanced and reduced, respectively, cell proliferation, as assessed by MTT analysis. (C) The overexpression of miR-221-3p and miR-375 in HepG2.2.15 cells increased and decreased, respectively, the level HBV-DNA, as demonstrated by qRT-PCR. (D) The overexpression of miR-221-3p and miR-375 downregulated and upregulated, respectively, TP53 expression, as assessed by western blotting. (E) and (F) Analysis of the co-expression of miR-221-3p/TP53 (E) and miR-375/TP53 (F) in HCC clinical tissue samples using starBase online software. The expression of both miR-221-3p and miR-375 was positively correlated with TP53 expression ($r = 0.313$ and P -value = $7.16E-10$ for miR-221-3p; $r = 0.036$ and P -value = $4.95E-01$ for miR-375). The two-independent t -test was used to compare the difference of miRNA relative expression, MTT, and HBV-DNA. ** $P < 0.01$; *** $P < 0.001$.

Full-size DOI: 10.7717/peerj.9100/fig-5

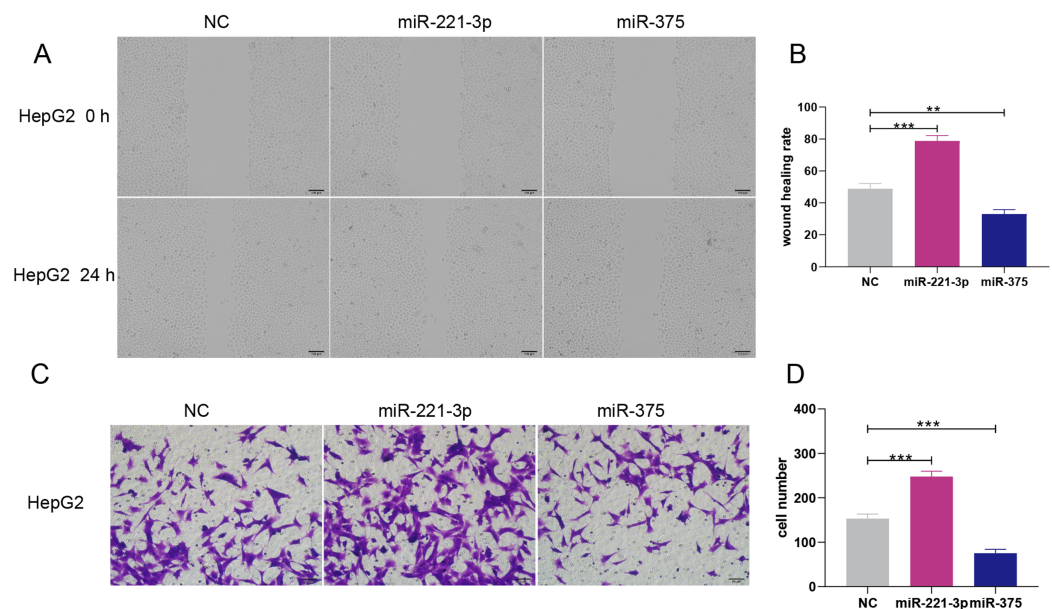


Figure 6 Overexpression of miR-221-3p and miR-375 enhanced and suppressed, respectively, the migration and invasion of HepG2 cell lines. (A) The wound healing assay was performed after transfection with NC, miR-221-3p mimic (50 nM), or miR-375 mimic (50 nM), and an additional 24 h of culture (picture magnification: 100 \times ; black bar: 100 μ m); HepG2 transfected with miR-221-3p and miR-375 mimics exhibited higher and lower migration ability compared to NC-transfected cells, respectively. (B) Quantification from A. (C) The transwell assay was performed after transfection with NC, miR-221-3p mimic (50 nM) or miR-375 mimic (50 nM) and an additional 24 h of culture (picture magnification: 200 \times ; black bar: 50 μ m). HepG2 transfected with miR-221-3p miR-375 mimics were more and less invasive compared to those transfected with NC, respectively. (D) Quantification from C. The two-independent *t*-test was used to compare the difference of wound healing rate and cell number. ***P* < 0.01; ****P* < 0.001. [Full-size](#) DOI: 10.7717/peerj.9100/fig-6

invasion were verified by a transwell assay, which demonstrated that miR-221-3p and miR-375 overexpression enhanced and inhibited, respectively, HepG2 cell invasion (Figs. 6C and 6D). In summary, the data confirmed that miR-221-3p and miR-375 are potential regulators of *TP53* expression, and could therefore affect HBV-DNA replication, as well as HCC cell proliferation, migration, and invasion.

DISCUSSION

The pathogenesis HCC is still unclear, and the known etiological factors mainly include exogenous factors, such as hepatitis virus infection, and endogenous factors, such as excessive drinking, metabolic disorders, and environmental factors (Kokudo *et al.*, 2019). The 5-year survival of HCC patients can be higher than 50% after early diagnosis (Forner, Llovet & Bruix, 2012). However, due to delayed diagnosis, most HCC patients are not suitable for further treatment and often have a poor prognosis.

Numerous studies had demonstrated that miRNAs play an important role in various biological processes of HCC cells, such as cell proliferation, HBV persistent infection, tumor suppressor genes expression, and metastasis. In China, the persistent exacerbation of HBV amplification is the main determinant of HCC recurrence (Yanming *et al.*, 2019). A recent study showed that miR-146a SNP (C/G) is associated with the susceptibility

to HBV infection and with spontaneous viral clearance ([Khanizadeh et al., 2019](#)). *TP53* mutation, the most common mutation in HCC, affects the progression and prognosis of HCC ([Long et al., 2019](#)). Interestingly, miR-487a stimulates cancer cell proliferation via PIK3R1-mediated AKT signaling and promotes metastasis via SPRED2-induced mitogen-activated protein kinase signaling in HCC ([Chang et al., 2017](#)). Hence, it is urgent need to systematically analyzed and experimentally verified the role of specific miRNAs in HBV amplification, as well as in the proliferation, migration, and invasion of HCC cells.

In this study, a data-driven decision was applied to gradually narrow down the scope of experimental verification miRNAs ([Lou et al., 2018](#)). First, we screened 20 upregulated and 30 downregulated miRNAs on the basis of the miRNA expression profiles of the [GSE108724](#) dataset. Subsequently, potential miRNA target genes were predicted for the top three upregulated and downregulated miRNAs ranked by $|\log_2FC|$. According to the results of GO and KEGG analysis, the identified miRNAs were implicated in focal adhesion, cell cycle regulation, HBV infection, and mitosis. Next, the top ten hub genes, ranked by degrees, of upregulated and downregulated miRNAs were identified. The generated miRNA-hub gene network showed that miR-221-3p and miR-375 modulated most of the hub genes. Moreover, the two latter miRNAs exhibited the highest score regarding *TP53* regulation. However, as far as we know, the effect of *TP53* expression modulated by miR-221-3p and miR-375 on the proliferation, invasion, metastasis, and HBV replication in HCC have rare been reported. It is of great significance to clarify the mechanism how the two miRNAs regulate the above phenotypes of HCC.

The present study confirmed that the expression of miR-221-3p and miR-375 was significantly upregulated and downregulated, respectively, in both HCC cell lines and HCC tissue samples. The upregulation of miR-212-3p and miR-375 enhanced and inhibited, respectively, HBV-DNA replication and amplification, as well as HCC cell migration and invasion. In addition, the upregulation of miR-212-3p and miR-375 exerted opposite effects on *TP53* expression, respectively suppressing and promoting its transcription. Recent studies have demonstrated that miR-221-3p functions as an oncogene in specific types of human cancer, including HCC ([Wang et al., 2019](#)), non-small cell lung cancer ([Yin, Zhang & Li, 2019](#)), glioma ([Milani et al., 2019](#)), gastric cancer ([Zhang et al., 2019](#)) and breast cancer ([Deng et al., 2017](#)). It was also reported that miR-375 inhibits the proliferation and migration of many cancer cells ([Guo et al., 2018](#); [Shen et al., 2014](#); [Wu et al., 2017](#)). Moreover, miR-221 promotes HCC cell migration by regulating the expression of plant homeodomain finger 2 (*PHF2*), which was demonstrated to be a target gene of miR-221 ([Fu et al., 2019](#)). Furthermore, *PHF2* acts as a vital regulator of cancer development in association with *TP53*, and is required for *TP53*-mediated cell death ([Lee et al., 2015](#)). Several studies demonstrated that miR-375 negatively regulates epithelial-mesenchymal transition, apoptosis, and cell migration by directly blocking its target, YWHAZ or ErbB2 in HCC cells ([Li, Jia & Ding, 2018](#); [Zhao et al., 2018](#)). A potent oncogenic cooperation between mutant *TP53* and *ErbB2* was also demonstrated in human Her2-positive breast cancer ([Li & Marchenko, 2017](#)). On the basis of our findings, we reasoned that, in association with miR-221-3p and miR-375, *TP53* could act as a tumor

suppressor by inhibiting HBV replication, proliferation, migration, and invasion of HCC cells, and promote p53-mediated cell apoptosis.

Unfortunately, there are some limitations in this study. First, despite the fact that the unvalidated microRNAs had a similar numbers of targets to the validated microRNAs, only the two miRNAs with significant variation were selected and further analyzed. Moreover, a dual-luciferase reporter experiment was not performed to directly verify whether *TP53* was the target gene of miR-221-3p and miR-375. The latter aspect will be the focus of forthcoming research in our laboratory.

CONCLUSIONS

In sum, we demonstrated that the aberrant expression of miR-221-3p and miR-375 may affect HBV-DNA replication, as well as the proliferation, migration, and invasion of HCC cells, possibly by modulating the expression of *TP53*. Thus, these two miRNAs may serve as crucial biomarkers for HCC diagnosis and prognosis.

ACKNOWLEDGEMENTS

I would like to thank professor Xin-guang Liu for his valuable suggestions on the design of the present study.

ADDITIONAL INFORMATION AND DECLARATIONS

Funding

This work was supported by the National Natural Science Foundation of China (Nos. 81671399 and 81971329), Guangdong Medical Research Fund (No. B2018262), Shaoguan Health Bureau Research Fund (No. Y19042), Shaoguan Science and Technology Fund (No. 2018sn095) and Outstanding Research Fund of YueBei People's Hospital, Natural Science Foundation of Guangdong Province, China (No. 2016A030307031). The funders had no role in study design, data collection and analysis, decision to publish, or preparation of the manuscript.

Grant Disclosures

The following grant information was disclosed by the authors:
National Natural Science Foundation of China: 81671399 and 81971329.
Guangdong Medical Research Fund: B2018262.
Shaoguan Health Bureau Research Fund: Y19042.
Shaoguan Science and Technology Fund: 2018sn095.
YueBei People's Hospital.
Natural Science Foundation of Guangdong Province, China: 2016A030307031.

Competing Interests

The authors declare that they have no competing interests.

Author Contributions

- Yanming Liu conceived and designed the experiments, performed the experiments, analyzed the data, prepared figures and/or tables, authored or reviewed drafts of the paper, and approved the final draft.
- Yue Cao performed the experiments, analyzed the data, prepared figures and/or tables, authored or reviewed drafts of the paper, and approved the final draft.
- Wencan Cai analyzed the data, prepared figures and/or tables, authored or reviewed drafts of the paper, and approved the final draft.
- Liangyin Wu analyzed the data, prepared figures and/or tables, authored or reviewed drafts of the paper, and approved the final draft.
- Pingsen Zhao conceived and designed the experiments, analyzed the data, authored or reviewed drafts of the paper, and approved the final draft.
- Xin-guang Liu conceived and designed the experiments, analyzed the data, prepared figures and/or tables, authored or reviewed drafts of the paper, and approved the final draft.

Human Ethics

The following information was supplied relating to ethical approvals (i.e., approving body and any reference numbers):

YueBei People's Hospital granted Ethical approval to carry out the study within its facilities (sumc-irb-2017).

Data Availability

The following information was supplied regarding data availability:

The raw measurements are available in the [Supplemental Files](#).

Supplemental Information

Supplemental information for this article can be found online at <http://dx.doi.org/10.7717/peerj.9100#supplemental-information>.

REFERENCES

- Chandrashekar DS, Bashel B, Balasubramanya SAH, Creighton CJ, Ponce-Rodriguez I, Chakravarthi B, Varambally S. 2017. UALCAN: a portal for facilitating tumor subgroup gene expression and survival analyses. *Neoplasia* **19**(8):649–658
DOI 10.1016/j.neo.2017.05.002.
- Chang RM, Xiao S, Lei X, Yang H, Fang F, Yang LY. 2017. miRNA-487a promotes proliferation and metastasis in hepatocellular carcinoma. *Clinical Cancer Research* **23**(10):2593–2604
DOI 10.1158/1078-0432.CCR-16-0851.
- Chin CH, Chen SH, Wu HH, Ho CW, Ko MT, Lin CY. 2014. cytoHubba: identifying hub objects and sub-networks from complex interactome. *BMC Systems Biology* **8**(Suppl. 4):S11
DOI 10.1186/1752-0509-8-S4-S11.
- Chou CH, Shrestha S, Yang CD, Chang NW, Lin YL, Liao KW, Huang WC, Sun TH, Tu SJ, Lee WH, Chiew MY, Tai CS, Wei TY, Tsai TR, Huang HT, Wang CY, Wu HY, Ho SY, Chen PR, Chuang CH, Hsieh PJ, Wu YS, Chen WL, Li MJ, Wu YC, Huang XY, Ng FL, Buddhakosai W, Huang PC, Lan KC, Huang CY, Weng SL, Cheng YN, Liang C, Hsu WL,

- Huang HD. 2018.** miRTarBase update 2018: a resource for experimentally validated microRNA-target interactions. *Nucleic Acids Research* **46(D1)**:D296–D302 DOI [10.1093/nar/gkx1067](https://doi.org/10.1093/nar/gkx1067).
- Da Huang W, Sherman BT, Lempicki RA. 2009a.** Bioinformatics enrichment tools: paths toward the comprehensive functional analysis of large gene lists. *Nucleic Acids Research* **37(1)**:1–13 DOI [10.1093/nar/gkn923](https://doi.org/10.1093/nar/gkn923).
- Da Huang W, Sherman BT, Lempicki RA. 2009b.** Systematic and integrative analysis of large gene lists using DAVID bioinformatics resources. *Nature Protocols* **4(1)**:44–57 DOI [10.1038/nprot.2008.211](https://doi.org/10.1038/nprot.2008.211).
- Davis S, Meltzer PS. 2007.** GEOquery: a bridge between the Gene Expression Omnibus (GEO) and BioConductor. *Bioinformatics* **23(14)**:1846–1847 DOI [10.1093/bioinformatics/btm254](https://doi.org/10.1093/bioinformatics/btm254).
- Deng L, Lei Q, Wang Y, Wang Z, Xie G, Zhong X, Wang Y, Chen N, Qiu Y, Pu T, Bu H, Zheng H. 2017.** Downregulation of miR-221-3p and upregulation of its target gene PARP1 are prognostic biomarkers for triple negative breast cancer patients and associated with poor prognosis. *Oncotarget* **8(65)**:108712–108725 DOI [10.18632/oncotarget.21561](https://doi.org/10.18632/oncotarget.21561).
- Edgar R, Domrachev M, Lash AE. 2002.** Gene expression omnibus: NCBI gene expression and hybridization array data repository. *Nucleic Acids Research* **30(1)**:207–210 DOI [10.1093/nar/30.1.207](https://doi.org/10.1093/nar/30.1.207).
- Forner A, Llovet JM, Bruix J. 2012.** Hepatocellular carcinoma. *Lancet* **379(9822)**:1245–1255 DOI [10.1016/S0140-6736\(11\)61347-0](https://doi.org/10.1016/S0140-6736(11)61347-0).
- Fu Y, Liu M, Li F, Qian L, Zhang P, Lv F, Cheng W, Hou R. 2019.** MiR-221 promotes hepatocellular carcinoma cells migration via targeting PHF2. *BioMed Research International* **2019**:4371405 DOI [10.1155/2019/4371405](https://doi.org/10.1155/2019/4371405).
- Guo J, Liu X, Yang Y, Liang M, Bai C, Zhao Z, Sun B. 2018.** miR-375 down-regulation of the rearranged L-myc fusion and hypoxia-induced gene domain protein 1A genes and effects on Sertoli cell proliferation. *Asian-Australasian Journal of Animal Sciences* **31(8)**:1103–1109 DOI [10.5713/ajas.17.0338](https://doi.org/10.5713/ajas.17.0338).
- Kanehisa M, Furumichi M, Tanabe M, Sato Y, Morishima K. 2017.** KEGG: new perspectives on genomes, pathways, diseases and drugs. *Nucleic Acids Research* **45(D1)**:D353–D361 DOI [10.1093/nar/gkw1092](https://doi.org/10.1093/nar/gkw1092).
- Khanizadeh S, Hasanvand B, Nikoo HR, Anbari K, Adhikary H, Shirkhani S, Lashgarian HE. 2019.** Association between miRNA-146a rs2910164 (G/C) polymorphism with the susceptibility to chronic HBV infection and spontaneous viral clearance in an Iranian population. *Journal of Medical Virology* **91(6)**:1063–1068 DOI [10.1002/jmv.25394](https://doi.org/10.1002/jmv.25394).
- Kokudo N, Takemura N, Hasegawa K, Takayama T, Kubo S, Shimada M, Nagano H, Hatano E, Izumi N, Kaneko S, Kudo M, Iijima H, Genda T, Tateishi R, Torimura T, Igaki H, Kobayashi S, Sakurai H, Murakami T, Watadani T, Matsuyama Y. 2019.** Clinical practice guidelines for hepatocellular carcinoma: The Japan Society of Hepatology 2017 (4th JSH-HCC guidelines) 2019 update. *Hepatology Research* **49(10)**:1109–1113 DOI [10.1111/hepr.13411](https://doi.org/10.1111/hepr.13411).
- Lee KH, Park JW, Sung HS, Choi YJ, Kim WH, Lee HS, Chung HJ, Shin HW, Cho CH, Kim TY, Li SH, Youn HD, Kim SJ, Chun YS. 2015.** PHF2 histone demethylase acts as a tumor suppressor in association with p53 in cancer. *Oncogene* **34**:2897–2909 DOI [10.1038/onc.2014.219](https://doi.org/10.1038/onc.2014.219).
- Li L, Jia L, Ding Y. 2018.** Upregulation of miR-375 inhibits human liver cancer cell growth by modulating cell proliferation and apoptosis via targeting ErbB2. *Oncology Letters* **16**:3319–3326 DOI [10.3892/ol.2018.9011](https://doi.org/10.3892/ol.2018.9011).

- Li JH, Liu S, Zhou H, Qu LH, Yang JH. 2014. starBase v2.0: decoding miRNA-ceRNA, miRNA-ncRNA and protein-RNA interaction networks from large-scale CLIP-Seq data. *Nucleic Acids Research* 42(D1):D92–D97 DOI 10.1093/nar/gkt1248.
- Li D, Marchenko ND. 2017. ErbB2 inhibition by lapatinib promotes degradation of mutant p53 protein in cancer cells. *Oncotarget* 8(4):5823–5833 DOI 10.18632/oncotarget.12878.
- Long J, Wang A, Bai Y, Lin J, Yang X, Wang D, Yang X, Jiang Y, Zhao H. 2019. Development and validation of a TP53-associated immune prognostic model for hepatocellular carcinoma. *EBioMedicine* 42:363–374 DOI 10.1016/j.ebiom.2019.03.022.
- Lou W, Chen J, Ding B, Chen D, Zheng H, Jiang D, Xu L, Bao C, Cao G, Fan W. 2018. Identification of invasion-metastasis-associated microRNAs in hepatocellular carcinoma based on bioinformatic analysis and experimental validation. *Journal of Translational Medicine* 16(1):266 DOI 10.1186/s12967-018-1639-8.
- Mantione KJ, Kream RM, Kuzelova H, Ptacek R, Raboch J, Samuel JM, Stefano GB. 2014. Comparing bioinformatic gene expression profiling methods: microarray and RNA-Seq. *Medical Science Monitor Basic Research* 20:138–142 DOI 10.12659/MSMBR.892101.
- Marangos P. 2016. Preparation of cell lysate from mouse oocytes for western blotting analysis. In: Nezis I, ed. *Oogenesis: Methods in Molecular Biology*. Vol. 1457. New York: Humana Press, 209–215.
- Milani R, Brognara E, Fabbri E, Manicardi A, Corradini R, Finotti A, Gasparello J, Borgatti M, Cosenza LC, Lampronti I, Dececchi MC, Cabrini G, Gambari R. 2019. Targeting miR-155-5p and miR-221-3p by peptide nucleic acids induces caspase-3 activation and apoptosis in temozolomide-resistant T98G glioma cells. *International Journal of Oncology* 55:59–68 DOI 10.3892/ijo.2019.4810.
- Ritchie ME, Phipson B, Wu D, Hu Y, Law CW, Shi W, Smyth GK. 2015. Limma powers differential expression analyses for RNA-sequencing and microarray studies. *Nucleic Acids Research* 43(7):e47 DOI 10.1093/nar/gkv007.
- Shannon P, Markiel A, Ozier O, Baliga NS, Wang JT, Ramage D, Amin N, Schwikowski B, Ideker T. 2003. Cytoscape: a software environment for integrated models of biomolecular interaction networks. *Genome Research* 13:2498–2504 DOI 10.1101/gr.1239303.
- Shen ZY, Zhang ZZ, Liu H, Zhao EH, Cao H. 2014. miR-375 inhibits the proliferation of gastric cancer cells by repressing ERBB2 expression. *Experimental and Therapeutic Medicine* 7:1757–1761 DOI 10.3892/etm.2014.1627.
- Szklarczyk D, Gable AL, Lyon D, Junge A, Wyder S, Huerta-Cepas J, Simonovic M, Doncheva NT, Morris JH, Bork P, Jensen LJ, Mering CV. 2019. STRING v11: protein–protein association networks with increased coverage, supporting functional discovery in genome-wide experimental datasets. *Nucleic Acids Research* 47:D607–D613 DOI 10.1093/nar/gky1131.
- Wang X, Liao X, Huang K, Zeng X, Liu Z, Zhou X, Yu T, Yang C, Yu L, Wang Q, Han C, Zhu G, Ye X, Peng T. 2019. Clustered microRNAs hsa-miR-221-3p/hsa-miR-222-3p and their targeted genes might be prognostic predictors for hepatocellular carcinoma. *Journal of Cancer* 10:2520–2533 DOI 10.7150/jca.29207.
- Wang T, Xu H, Qi M, Yan S, Tian X. 2018. miRNA dysregulation and the risk of metastasis and invasion in papillary thyroid cancer: a systematic review and meta-analysis. *Oncotarget* 9:5473–5479 DOI 10.18632/oncotarget.16681.
- Wong NW, Chen Y, Chen S, Wang X. 2018. OncomiR: an online resource for exploring pan-cancer microRNA dysregulation. *Bioinformatics* 34:713–715 DOI 10.1093/bioinformatics/btx627.

- Wu Y, Sun X, Song B, Qiu X, Zhao J. 2017.** MiR-375/SLC7A11 axis regulates oral squamous cell carcinoma proliferation and invasion. *Cancer Medicine* **6**(7):1686–1697 DOI [10.1002/cam4.1110](https://doi.org/10.1002/cam4.1110).
- Xie S, Jiang X, Zhang J, Xie S, Hua Y, Wang R, Yang Y. 2019.** Identification of significant gene and pathways involved in HBV-related hepatocellular carcinoma by bioinformatics analysis. *PeerJ* **7**:e7408 DOI [10.7717/peerj.7408](https://doi.org/10.7717/peerj.7408).
- Yanming L, Yue C, Wencan C, Liangyin WU, Xijun L, Jiafeng Z, Fengping HE. 2019.** Combined detection of AFP-L3, GP73 and TIP30 enhances diagnostic accuracy for HBV-related cirrhosis and hepatocellular carcinoma. *Journal of the Pakistan Medical Association* **69**:1279–1286.
- Yin G, Zhang B, Li J. 2019.** miR-221-3p promotes the cell growth of non-small cell lung cancer by targeting p27. *Molecular Medicine Reports* **20**:604–612 DOI [10.3892/mmr.2019.10291](https://doi.org/10.3892/mmr.2019.10291).
- Zha Y, Yao Q, Liu JS, Wang YY, Sun WM. 2018.** Hepatitis B virus X protein promotes epithelial-mesenchymal transition and metastasis in hepatocellular carcinoma cell line HCCLM3 by targeting HMGA2. *Oncology Letters* **16**:5709–5714 DOI [10.3892/ol.2018.9359](https://doi.org/10.3892/ol.2018.9359).
- Zhang Y, Huang H, Zhang Y, Liao N. 2019.** Combined detection of serum MiR-221-3p and MiR-122-5p expression in diagnosis and prognosis of gastric cancer. *Journal of Gastric Cancer* **19**(3):315–328 DOI [10.5230/jgc.2019.19.e28](https://doi.org/10.5230/jgc.2019.19.e28).
- Zhang X, Kang C, Li N, Liu X, Zhang J, Gao F, Dai L. 2019.** Identification of special key genes for alcohol-related hepatocellular carcinoma through bioinformatic analysis. *PeerJ* **7**(6):e6375 DOI [10.7717/peerj.6375](https://doi.org/10.7717/peerj.6375).
- Zhao JF, Zhao Q, Hu H, Liao JZ, Lin JS, Xia C, Chang Y, Liu J, Guo AY, He XX. 2018.** The ASH1-miR-375-YWHAZ signaling axis regulates tumor properties in hepatocellular carcinoma. *Molecular Therapy - Nucleic Acids* **11**:538–553 DOI [10.1016/j.omtn.2018.04.007](https://doi.org/10.1016/j.omtn.2018.04.007).
- Zhu HR, Yu XN, Zhang GC, Shi X, Bilegsaikhan E, Guo HY, Liu LL, Cai Y, Song GQ, Liu TT, Dong L, Janssen HLA, Weng SQ, Wu J, Shen XZ, Zhu JM. 2019.** Comprehensive analysis of long noncoding RNAmessenger RNAmicroRNA coexpression network identifies cell cyclereLATED lncRNA in hepatocellular carcinoma. *International Journal of Molecular Medicine* **44**:1844–1854 DOI [10.3892/ijmm.2019.4323](https://doi.org/10.3892/ijmm.2019.4323).